Irreversible electrical resistivity and unstable bonding nature in the fast-Li-ion conductor β-LiGa

K. Kuriyama, H. Hamanaka, and R. Taguchi
College of Engineering and Research Center of Ion Beam Technology, Hosei University, Koganei, Tokyo 184, Japan

M. Yahagi
Faculty of Engineering, Aomori University, Aomori 030, Japan
(Received 13 March 1997)

The temperature-dependent electrical resistivity above 300 K of β-LiGa [NaTl structure (space group $Fd3m$)] is presented. An irreversible behavior of electrical resistivity was observed in the Li excess β-LiGa. An abrupt decrease in electrical resistivity is associated with the decrease of effective scatterers arising from the disappearance of Li antisite defects (Li_{Ga}) with an activation energy of 0.57 ± 0.02 eV at elevated temperatures. These results suggest the existence of an unstable bonding resulting from the relaxation of sp^3-like Ga bond, at Li_{Ga}. [S0163-1829(97)03543-1]

The intermetallic compound β-LiGa has been considered as possible electrode material because of its high diffusion coefficient for the Li ion.[1] β-LiGa [NaTl structure,[2] space group $Fd3m$] is composed of two interpenetrating sublattices, each forming a diamond lattice (Fig. 1). A theoretical investigation[3] showed that the bonding in the ideal β phase is dominated by the attractive potential of the Ga ions and is described in terms of a sp^3-like bond arising from an electron transfer from Li to Ga. The defect structure[4] in the β phase has been associated with a large, constitutional, vacancy concentration on the Li sublattice, since β-LiGa has both a homogeneity range[4,5] of approximately 44–54 at. % Li and a relatively low activation energy (0.15 eV) (Ref. 6) for diffusion of Li. The defect structure at room temperature consists of two types of defects, vacancies in the lithium sublattice (V_{Li}), and lithium antistructure atoms in the gallium sublattice (Li_{Ga}). This defect structure has been inferred from measurements of the lattice parameter and density, rather than directly from scattering methods. The V_{Li} concentration decreases from about 11.5 at. % to about 2.0 at. % with increasing Li content C_{Li}, while the Li_{Ga} concentration varies from 0 to about 5 at. % with increasing C_{Li}. The resistivity of β-LiGa is strongly affected by the Li composition.[4,7] The room-temperature resistivity varies from about 15 to about 100 $\mu\Omega$ cm with increasing C_{Li}. This characteristic is mainly dominated by the existence of the Li_{Ga} antisite defects, since the Li atom (valence+1) on the Ga site (valence+3), Li_{Ga} (valence−2), is much more effective[4] as a scatterer for carriers other than V_{Li} (valence −1). According to Linde's rule,[8] the resistivity of a metal containing charged impurities is proportional to the square of the valence difference between the impurity and matrix atoms. The motion of Li in the mixed-conductor β-LiGa would also be related to the defect structure containing V_{Li}. Indeed, an anomalous electrical resistivity[4,7] observed at around 230 K has been associated with the ordering of vacancies on the Li sublattice as well as the V_{Li} ordering in β-LiAl.[9,10] However, the electrical conduction above room temperature has not been investigated for β-LiGa. In order to understand the motion of Li in β phase as an ionic conductor, it is required to study the conduction mechanism relating to V_{Li} and Li_{Ga} at elevated temperatures.

In this paper, we report an irreversible electrical resistivity in β-LiGa and discuss the origin of the anomalous resistivity taking into account the defect structure. We also suggest the existence of an unstable bonding around the Li_{Ga} antisite defect.

The details of the sample preparation have already been reported.[4] The Li content C_{Li} was estimated with an accuracy of ±0.5 at. % from the relation of lattice parameter (or room-temperature resistivity) versus composition.[4] Also, the Li content was followed up by atomic-absorption spectroscopy. The resistivity measurements were carried out using a Van der Pauw method used for β-LiGa.[11] A typical thickness of samples used here was about 1 mm. Electrical contact was made by pointed tungsten probes pressing into the top face of the sample at each of its four corners. The dc current of 200 mA from a current source (Keithley 228A) was supplied to the sample during the resistivity measurements. The in-

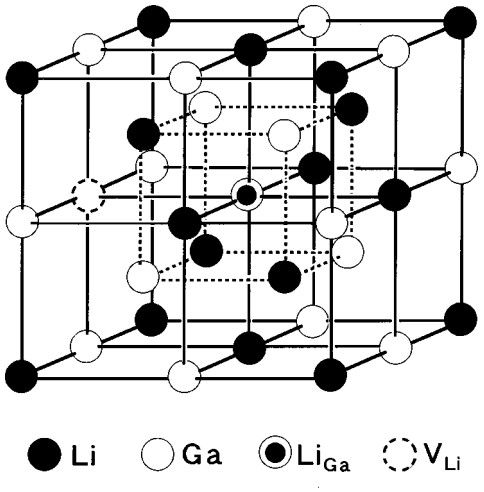

FIG. 1. Crystal structure of β-LiGa (NaTl-type) containing a Li-vacancy and a Li antisite defect.

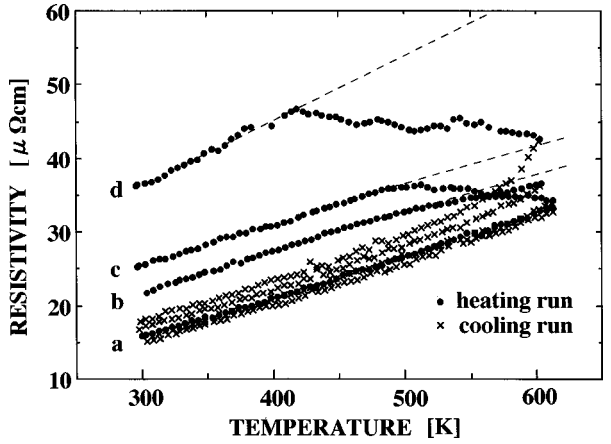

FIG. 2. Temperature-dependent electrical resistivities for various Li compositions of β-LiGa. Samples are as follows: (a) (43.5 at. % Li, $V_{\mathrm{Li}}\sim 11.5$ at. %, and $\mathrm{Li}_{\mathrm{Ga}}=0$ at. %); (b) (46.5 at. % Li, $V_{\mathrm{Li}}\sim 7.5$ at. %, and $\mathrm{Li}_{\mathrm{Ga}}\sim 0.5$ at. %); (c) (47.0 at. % Li, $V_{\mathrm{Li}}\sim 7.0$ at. %, and $\mathrm{Li}_{\mathrm{Ga}}\sim 0.7$ at. %); and (d) (48.0 at. % Li, $V_{\mathrm{Li}}\sim 5.5$ at. %, and $\mathrm{Li}_{\mathrm{Ga}}\sim 1.0$ at. %). Dashed lines represent the $\rho_i+\rho_l(T)$ term extrapolated using experimental values in heating run, where ρ_i and $\rho_l(T)$ are terms relating to the intrinsic defects and the linear-phonon term, respectively.

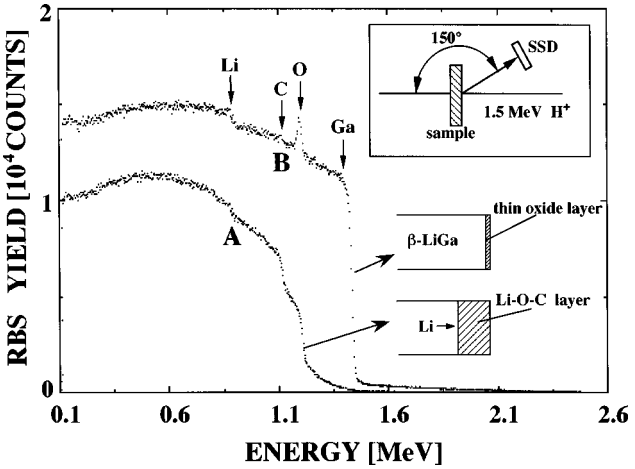

FIG. 3. RBS spectra taken after the resistivity measurements. 1.5 MeV H^+ beams were used. *A* and *B* represent RBS spectra before and after the elimination of the surface layer, respectively.

duced voltages were measured with a nanovoltmeter (Keithley 148). The electrical measurements were carried out under a flow of Ar gas using a system constructed from the Pyrex glass tube, which was kept at about 1 atm. The samples were heated and cooled at a rate of about 100 °C/h. Elements contained in the surface products after the resistivity measurements were examined by Rutherford backscattering spectrometry (RBS) using a proton beam of 1.5 MeV.

Temperature-dependent electrical resistivities for various Li compositions are shown in Fig. 2. The resistivity at Li-deficient phase boundary ($\sim$43.5 at. % Li; curve *a* in Fig. 2) showed the monotonic variation in heating and cooling runs, indicating the reversible behavior. The β-phase boundary contains the V_{Li} defects of about 11.5 at. %, but not the $\mathrm{Li}_{\mathrm{Ga}}$ antisite defects. On the other hand, the resistivity of β phase with the excess Li concentrations showed the irreversible behavior in heating and cooling runs. As shown in Fig. 2 (curve *b*), for a sample ($V_{\mathrm{Li}}\sim 7.5$ at. % and $\mathrm{Li}_{\mathrm{Ga}}\sim 0.5$ at. %) with $C_{\mathrm{Li}}\sim 46.5$ at. %, the resistivity in heating run begins to drop at around 500 K and reaches that of the β-phase boundary at around 620 K. In the cooling run, the resistivity decreases along with that of the β-phase boundary. The resistivity drop shifts to lower temperatures with increasing C_{Li}. In the cooling run, however, the Li-excess β-LiGa (curves *c* and *d* in Fig. 2) varied with a slightly larger resistivity, relative to the Li-deficient β-phase boundary. This would be attributed to the presence of the oxide layer observed on the surface of β-LiGa as discussed later. In particular, the oxidation was enhanced on the surface of the samples with the excess Li concentration, containing a large number of $\mathrm{Li}_{\mathrm{Ga}}$ defects. For the samples with $C_{\mathrm{Li}}>48$ at. %, it was difficult to measure the resistivity because of the unstable electromotive force.

Elements in the oxide layer were examined by the RBS experiments using a proton beam. Figure 3 shows the RBS spectra taken before and after the elimination of the surface layer. The RBS data showed that the oxide layer consists of a Li-C-O compound. After the elimination of the oxide layer, the RBS spectrum consisted of the Li and Ga signals from the β-LiGa except the very thin oxide layer. This thin layer was grown during the setting of the sample into the RBS instrument. The presence of the oxide layer suggests that the irreversible behavior of electrical resistivity arises from the out-diffusion of Li ions moving into the surface from the interior of the crystal. Since Li ions in the oxide layer cannot easily move into the interior of the crystal, β-LiGa in a cooling run is deficient in Li content. As a result, the irreversible behavior in electrical resistivity occurs in β-LiGa. A similar behavior has been observed in β-LiAl.[11,12] Furthermore, the corrosive reaction between the tungsten probes and the oxide layer was enhanced according as C_{Li} increases, inducing the undesirable electromotive force.

In order to understand the mechanism of anomalous resistivity, we should pay attention to the Li diffusion from $\mathrm{Li}_{\mathrm{Ga}}$ sites rather than from $\mathrm{Li}_{\mathrm{Li}}$ sites, since an anomalous behavior at Li-deficient phase boundary ($\mathrm{Li}_{\mathrm{Ga}}=0$ at. %) is not distinguishable as shown in Fig. 2. Although Ga vacancies (V_{Ga}) are created by Li diffusion out of $\mathrm{Li}_{\mathrm{Ga}}$ sites through V_{Li}, V_{Ga} is filled up successively by Li migration from $\mathrm{Li}_{\mathrm{Li}}$ sites. $\mathrm{Li}_{\mathrm{Ga}}$ moving into the surface from the interior of the crystal would be incorporated into the oxide layer, resulting in an increase of V_{Li} sites in the crystal. As a result, the crystal reaches the Li-deficient β-phase boundary. In the Li migration process at elevated temperatures the rearrangement of Li and Ga atoms may be required to fill up V_{Ga} sites by Ga migration from $\mathrm{Ga}_{\mathrm{Li}}$ sites as seen in β-LiAl.[13] However, the presence of $\mathrm{Ga}_{\mathrm{Li}}$ antisites is not yet confirmed in β-LiGa. Therefore, the drop in electrical resistivity at elevated temperatures is attributed to mainly the disappearance of the $\mathrm{Li}_{\mathrm{Ga}}$ antisites in β phase with the excess Li concentration, since $\mathrm{Li}_{\mathrm{Ga}}$ behaves as a scatterer of the valence -2.

The variation of the electrical resistivity due to the vacancy-type defects has been evaluated for aluminum.[14] The resistivity increment ascribed to the vacancy-type defects was obtained by difference and can be represented by the expression of $\Delta\rho=\rho_0\exp(-E_f/kT)$, where E_f is the formation energy of monovacancy. Since in the case of

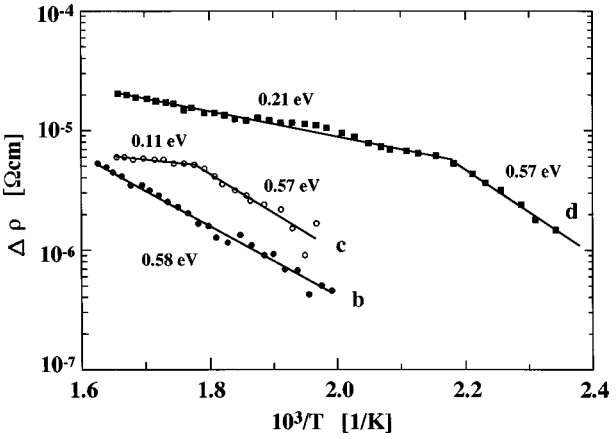

FIG. 4. Resistivity decrement $\Delta\rho$ vs T^{-1} plots. Curves b, c, and d correspond to the resistivities shown in Fig. 2.

β-LiGa the disappearance of cation-antisite defects induces the drop in resistivity, the individual contributions to the total resistivity (ρ_{total}) would be expressed using the resistivity (ρ_i) for the intrinsic defects, $\rho_l(T)$ for the linear-phonon term, and $\rho(\text{Li}_{\text{Ga}})$ for the exponential term for disappearing cation-antisite defects, namely, $\rho_{\text{total}}=\rho_i+\rho_l(T)+\rho(\text{Li}_{\text{Ga}})$. The linear part, $\rho_i+\rho_l(T)$, was extraporated using experimental values in heating run as depicted by a broken line in Fig. 2 and used as the baseline to determine the $\rho(\text{Li}_{\text{Ga}})$, namely, $\Delta\rho=[\rho_i+\rho_l(T)]-\rho_{\text{total}}=\rho(\text{Li}_{\text{Ga}})\propto\exp(-E_A/kT)$. The resulting plot of $\ln(\Delta\rho)$ versus $1/T$ is linear at low temperatures, with all samples yielding the same activation energy, attributed to vanishing Li_{Ga} (see Fig. 4). $E_A=0.57\pm0.02$ eV was observed in β-LiGa (46.5 at. % Li) near the β-phase boundary, while $\Delta\rho$ in β-LiGa (47.0 and 48.0 at. % Li) with the excess Li concentration varied with two straight lines with $E_A=0.57\pm0.02$ and 0.11–0.21 eV, respectively. The higher activation energy is attributed to the disappearance of Li_{Ga} as the effective scatterer for carriers, since the resistivity in cooling run coincides with that of Li-deficient β-phase boundary with $\text{Li}_{\text{Ga}}=0$ at. % Li (see curves a and b in Fig. 2). At higher Li concentrations, there is a crossover at higher T to a region with a lower activation. Although this behavior cannot be clearly explained at this stage, the lower activation energies may be correlated with the Li ion motion in the oxide layer, indicating a complex conduction mechanism consisting of both the oxide layer and the bulk crystal.

The presence of Li_{Ga} may relax the bonding arising from the attractive potential of the Ga ions,[3] indicating the unstable bonding of the Li ion in the Ga position resulting from the relaxation in a sp^3-like Ga bond at Li_{Ga} sites. The unstable bonding of Li_{Ga} sites might lead to the disappearance of Li_{Ga} defects at higher temperatures, resulting from the resistivity drop due to the reduction of the scatterer. It is supposed that the presence of large concentrations of Li_{Ga} antisite defects makes a shallower bonding state for the Li_{Ga}, leading to the release of the Li ions at progressively lower temperatures. As a result, the resistivity drop shifts to the low-temperature region with increasing Li_{Ga} concentration as seen in Fig. 2. Since the isolated Li_{Ga} in β-LiGa has four nearest-neighbor Li atoms as shown in Fig. 1, this situation can be seen as a Li cluster consisting of five Li atoms. Li at Ga sites may be released with an activation energy $E_A=0.57\pm0.02$ eV as V_{Li} comes up to a nearest-neighbor Li site at around Li_{Ga}. Further studies to confirm this argument are required.

In summary, we have presented the temperature-dependent electrical resistivity above 300 K of β-LiGa. An irreversible behavior of electrical resistivity was found in the Li-excess β-LiGa containing two types of defects, V_{Li} and Li_{Ga}, while it was not observed in Li-deficient β-phase boundary containing only the V_{Li} defects. An abrupt decrease in electrical resistivity was associated with the decrease of effective scatterers arising from the disappearance of Li_{Ga} with an activation energy of 0.57 ± 0.02 eV at elevated temperatures. The unstable bonding in β-LiGa was attributed to the lattice relaxation in a sp^3-like Ga bond at Li_{Ga}.

The present work was supported in part by Grant-in-Aid for Scientific Research on Priority Areas (No. 260) from The Ministry of Education, Science and Culture.

[1] C. J. Wen and R. A. Huggins, J. Electrochem. Soc. **128**, 1636 (1981).
[2] E. Zintl and G. Brauer, Z. Phys. Chem. Abt. B **20**, 245 (1933).
[3] J. Hafner and W. Jank, Phys. Rev. B **44**, 11 662 (1991).
[4] K. Kuriyama, H. Hamanaka, S. Kaidou, and M. Yahagi, Phys. Rev. B **54**, 6015 (1996).
[5] R. Thümmel and W. Klemm, Z. Anorg. Allg. Chem. **376**, 44 (1970).
[6] H. E. Schone and W. D. Knight, Acta Metall. **11**, 179 (1963).
[7] K. Kuriyama, K. J. Volin, T. O. Brun, and S. Susman, Phys. Rev. B **33**, 7291 (1986).
[8] For example, N. F. Mott and H. Jones, *The Theory of the Properties of Metals and Alloys* (Dover, New York, 1958), p. 292.
[9] K. Kuriyama, T. Kamijoh, and T. Nozaki, Phys. Rev. B **22**, 470 (1980); K. Kuriyama, S. Yanada, T. Nozaki, and T. Kamijoh, *ibid.* **24**, 6158 (1981).
[10] T. O. Brun, S. Susman, R. Dejus, B. Granelli, and K. Sköld, Solid State Commun. **45**, 721 (1983).
[11] K. Kuriyama, M. Yahagi, T. Nakaya, T. Ashida, K. Satoh, and K. Iwamura, Phys. Rev. B **29**, 5924 (1984).
[12] H. Sugai, M. Tanase, M. Yahagi, T. Ashida, H. Hamanaka, K. Kuriyama, and K. Iwamura, Phys. Rev. B **52**, 4050 (1995).
[13] T. O. Brun, J. D. Jorgensen, M. Misawa, F. J. Rotells, S. Susman, and D. F. R. Milder, J. Electrochem. Soc. **129**, 2509 (1982).
[14] R. O. Simmons and R. W. Balluffi, Phys. Rev. **117**, 62 (1960).